



8-Alkylmercaptocaffeine derivatives: antioxidant, molecular docking, and in-vitro cytotoxicity studies

Saman Sargazi^{a,*}, Sheida Shahraki^a, Omolbanin Shahraki^{b,**}, Farshid Zargari^{b,c}, Roghayeh Sheervalilou^b, Saeid Maghsoudi^d, Mohammad Navid Soltani Rad^d, Ramin Saravani^{a,e}

^a Cellular and Molecular Research Center, Resistant Tuberculosis Institute, Zahedan University of Medical Sciences, Zahedan, Iran

^b Pharmacology Research Center, Zahedan University of Medical Sciences, Zahedan, Iran

^c Department of Chemistry, Faculty of Science, University of Sistan and Baluchestan, Zahedan, Iran

^d Medicinal Chemistry Research Laboratory, Department of Chemistry, Shiraz University of Technology, Shiraz, Iran

^e Department of Clinical Biochemistry, School of Medicine, Zahedan University of Medical Sciences, Zahedan, Iran

ARTICLE INFO

Keywords:

Methylxanthines
Cytotoxicity
Antioxidant
cGMP
Molecular dynamics simulation
Molecular docking

ABSTRACT

Due to their unique pharmacological characteristics, methylxanthines are known as therapeutic agents in a fascinating range of medicinal scopes. In this report, we aimed to examine some biological effects of previously synthesized 8-alkylmercaptocaffeine derivatives. Cytotoxic and antioxidative activity of 8-alkylmercaptocaffeine derivatives were measured in malignant A549, MCF7, and C152 cell lines. Assessment of cGMP levels and caspase-3 activity were carried out using a colorimetric competitive ELISA kit. Computational approaches were employed to discover the inhibitory mechanism of synthesized compounds. Among the twelve synthesized derivatives, three compounds (C1, C5, and C7) bearing propyl, heptyl, and 3-methyl-butyl moieties showed higher and more desirable cytotoxic activity against all the studied cell lines ($IC_{50} < 100 \mu M$). Furthermore, C5 synergistically enhanced cisplatin-induced cytotoxicity in MCF-7 cells ($CI < 1$). Both C5 and C7 significantly increased caspase-3 activity and intracellular cGMP levels at specific time intervals in all studied cell lines ($P < 0.05$). However, these derivatives did not elevate LDH leakage ($P > 0.05$) and exhibited no marked ameliorating effects on oxidative damage ($P > 0.05$). Computational studies showed that H-bond formation between the nitrogen atom in pyrazolo[4,3-D] pyrimidine moiety with Gln817 and creating a hydrophobic cavity result in the stability of the alkyl group in the PDE5A active site. We found that synthesized 8-alkylmercaptocaffeine derivatives induced cell death in different cancer cells through the cGMP pathway. These findings will help us to get a deeper insight into the role of methylxanthines as useful alternatives to conventional cancer therapeutics.

1. Introduction

Derived from the purine base xanthine, methylxanthines are naturally found in berries, seeds, and leaves of many plants like coffee, cocoa, and tea [1,2]. The based scaffolds of these chemicals are well-recognized by different receptors and enzymes within cells; therefore, they were widely studied for their many pharmacological characteristics [3]. These unique molecules include the compounds caffeine (CAF), theobromine (found in chocolate), theophylline (found in tea), paraxanthine, pentoxifylline, aminophylline, 3-isobutyl-1-methylxanthine, and so on [1]. Lately, methylxanthine derivatives were widely examined for their

anti-allergic, anti-psychotic, antispasmodic, osteoprotective, cardio- tonic, anticancer, and other properties [4–6]. Yet, the site of alkylation mainly determines the biological effects of these compounds [4].

The cGMP signaling pathways are of broad biochemical and pathological significance. In this regard, the modulation of the intracellular cyclic nucleotides, including cAMP and cGMP, is considered a promising approach for cancer treatment [7]. As a second messenger, cGMP is inactivated by phosphodiesterase (PDE) enzymes. Accordingly, increased cGMP levels activate cGMP-dependent protein kinase (PKG), a protein kinase with decreased expression in cancer cells compared with normal cells [8]. Hence, agents that elevate cGMP levels through PDE

* Corresponding author.

** Corresponding author.

E-mail addresses: sgz.biomed@zaums.ac.ir (S. Sargazi), o.shahraki@gmail.com (O. Shahraki).

<https://doi.org/10.1016/j.bioorg.2021.104900>

Received 17 December 2020; Received in revised form 1 April 2021; Accepted 6 April 2021

Available online 9 April 2021

0045-2068/© 2021 Elsevier Inc. All rights reserved.

inhibition have gained much attention as potential anticancer therapeutics [9,10]. We previously showed that increasing intracellular cGMP levels might arrest growth and induce apoptotic cell death in breast cancer cells [11]. Various aromatic and heteroaromatic compounds have now been synthesized for effective inhibition of various PDEs. The ring is essential for mimicking the purine in the cN substrate and direct competition with cN for access to the catalytic site of the PDE enzymes [12]. Recent evidence has revealed that methylxanthines could effectively inhibit cyclic nucleotide (cN) PDEs [12]; thereby, being broadly in research and for the treatment of different diseases, including malignant cancers [13].

Recently, antioxidant effects have been proposed for methylxanthines. These chemicals considerably ameliorated reactive oxygen species (ROS)-induced oxidative damages *in vivo* and *in vitro* [14,15], mostly attributed to a scavenging activity towards hydroxyl radicals. Santos and colleagues showed that methylxanthine derivatives have higher antioxidant capacity than natural xanthines usually found in the human diet [16]. Moreover, it has been reported that chronic treatment with PDE inhibitors reduces oxidative stress and enhanced mitochondrial integrity [17,18].

Classic chemotherapeutic agents such as platinum-based drugs have shown limited success in cancer therapies due to their severe side effects [7]. To overcome this therapeutic obstacle, recent investigations were focused on targeted inhibition of signaling pathways using the platinum-based drug substitutes, aimed to decrease the drug resistance caused by these agents [19,20].

Previous studies indicated that methylxanthines induced protection against tumor cells [21,22] and also increased the sensitivity of tumor cells to alkylating agents [23,24]. Given all these observations, herein, we report the biological effects of previously synthesized 8-alkylmercaptocaffeine derivatives in different cancer cells [4]. We hypothesized that these compounds would exert antioxidant and cytotoxic effects while suppressing the cGMP signal transduction pathway. Our findings can provide a rationale for using these compounds as a beneficial alternative

strategy for cancer therapy.

2. Material and methods

2.1. Chemicals and assay kits

Six and 96-well cell culture plates were supplied by Sorfa (Zhejiang, China (Mainland)). Fetal bovine serum (FBS) was purchased from Biochrom (Berlin, Germany). Cisplatin, propidium iodide (PI), trypan blue, dimethylsulfoxide (DMSO), and 3-(4,5-Dimethylthiazol-2-yl)-2,5-diphenyltetrazolium bromide (MTT) powder were obtained from Sigma-Aldrich, USA. Phosphate buffered saline (PBS), antibiotic/antimycotic solution, and the trypsin-EDTA solution was procured from Innovative Biotech Co. (INOCOLON, Iran). The culture media, RPMI1640, and Dulbecco's Modified Eagle Medium (DMEM) were from Gibco (Rockville, MD, USA). All the other chemicals used were of technical grade and obtained from Merck Company.

2.2. Synthesized compounds

We previously synthesized twelve derivatives of 8-alkylmercaptocaffeine (Table 1) through a reaction shown in Scheme 1. For cisplatin or each derivative of 8-alkylmercaptocaffeine being tested, 20 mM stock solution was prepared in DMSO.

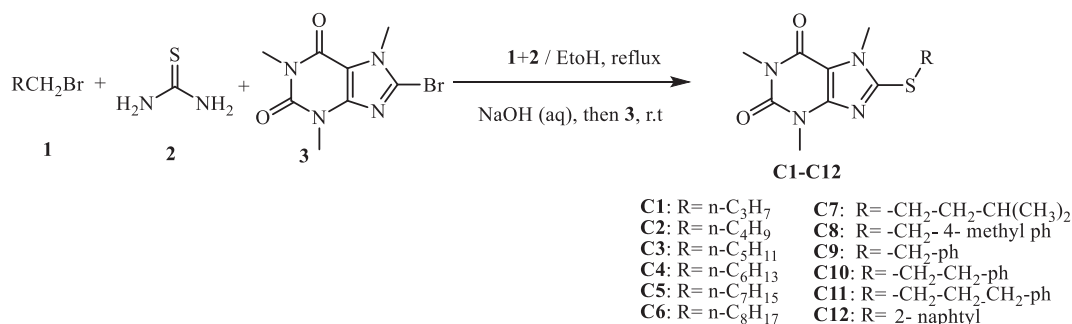
2.3. Cell culture

HUVEC (human umbilical vein endothelial cells), and MCF-7 (human breast adenocarcinoma), A549 (human lung adenocarcinoma), and KB (human oral epidermoid carcinoma) cell lines were obtained from the Pasteur Institute of Iran (Teheran, Iran) and tested negative for mycoplasma contamination. Cells were grown in RPMI1640 (MCF-7 and KB) and DMEM (A549 and HUVEC) medium supplemented with 10% FBS, amphotericin B (250 µg/mL), streptomycin (50 µg/mL),

Table 1
The molecular structure of 8- substituted alkylmercaptocaffeine derivatives.

Compound	MW	Compound	MW
C1	268.34	C7	296.39
C2	282.36	C8	330.40
C3	296.39	C9	316.38
C4	310.42	C10	330.40
C5	324.44	C11	344.43
C6	366.52	C12	366.44

MW: Molecular weight.



Scheme 1. The one-pot, three-component reaction of synthesis of 8-alkylmercaptocaffeines [4].

penicillin (50 U/mL) in a humidified atmosphere under the standard cell culture conditions (37 °C and 5% CO₂). Cells were detached from culture flasks using trypsin-EDTA (0.25%) and seeded in either 96-well or 6-well plates for the following experiments.

2.4. Cytotoxicity evaluation

The half-maximal inhibitory concentration (IC₅₀) of the previously synthesized 8-alkylmercaptocaffeine derivatives was examined using a tetrazolium-based colorimetric MTT assay [25]. 100 μL of the cell suspensions (5000 cells/well) were seeded and given 24 h to attach to the culture flask. Afterward, the culture medium was carefully discarded and replaced with a fresh medium containing increasing concentrations of the compounds (25–200 μM) or cisplatin (1–16 μM) and incubated for 72 h. Then, 20 μL of MTT (5 mg/ml) was placed into each microwell. After 4 h incubation at 37 °C, the medium was removed and replaced with 200 μL of DMSO. Plates were gently shaken for 25 min, and the absorbance was read at 570 nm using an ELISA reader (Spectra Max Gemini®, Molecular Devices). The IC₅₀ values were calculated via the CurveExpert program version 1.4 for Windows.

2.5. Analysis of combined drug effects

Analysis of multiple drug effects was done using Chou and Talalay methods according to a median-effect principle [26]. For this purpose, cells were simultaneously treated with 8-alkylmercaptocaffeine derivatives (C1, C5, and C7) and cisplatin, with fixed combination ratios. Increasing concentrations, each diluted 1:2, within the appropriate ranges were used. For each level of fraction affected (Fa), the combination index (CI) for indicating drug interactions was calculated using CompuSyn software (Version 1.0, Combo-Syn Inc., US) where CI < 1, CI = 1, and CI > 1 indicates synergism, additivity, and antagonism, respectively [27].

2.6. Lactate dehydrogenase leakage assay

As a marker of cell membrane integrity, LDH leakage was measured in the medium of cultured cells using a colorimetric lactate dehydrogenase (LDH) cytotoxicity assay kit (Cayman Chemical Company, Ann Arbor, MI, USA) according to the manufacturer's protocol. Cells (300 × 10⁵/well) were seeded in a 6-well microplate and incubated overnight. After treatment for 72 h, 100 μL of culture supernatant was added to a 96-well microplate for analysis. LDH leakage (% of total) is measured following the formula:

$$\left(\frac{OD_{\text{test}} - OD_{\text{spontaneous release}}}{OD_{\text{maximum release}} - OD_{\text{release}}} \right) \times 100,$$

OD_{test} is the absorbance of cells treated with 8-alkylmercaptocaffeine derivatives (C1, C5, and C7 equal to their IC₅₀ values), OD_{spontaneous release} is the absorbance of microwells containing assay buffer, and OD_{maximum release} represents the absorbance of microwells containing cells. Absorption was read at 540 nm against 592 nm as a background

using an ELISA reader (Spectra Max Gemini®, Molecular Devices).

2.7. Caspase-3 activity assay

To assess the cell activity of caspase-3, a marker of apoptosis, cells were seeded in 6-well plates above concentrations and treated with 8-alkylmercaptocaffeine derivatives (C1, C5, and C7 equal to their IC₅₀ values) for 24 h. Using a colorimetric commercial kit (R&D systems Co., Grodig, Germany) according to the manufacturer's instruction, the activity of caspase-3 was measured in cells supernatant.

2.8. Measurement of cGMP levels

The intracellular cGMP levels were quantitatively measured using a cGMP direct immunoassay kit (R&D Systems, Minneapolis, MN, USA), as previously described [28]. Briefly, cells were seeded in 6-well plates. After reaching confluency, cells were treated with 8-alkylmercaptocaffeine derivatives (C1, C5, and C7 equal to their IC₅₀ values) and incubated at room temperature at short (6 h) and long (24 h) time intervals. Then, cells were lysed, and the cell suspension was added into a 96-well plate coated with a goat anti-rabbit antibody. The plate was washed three times in PBS, and the substrate solution was added. Following a 30 min incubation at 37 °C, the stop solution was added. The absorbance was read at 450 nm using an ELISA reader (Spectra Max Gemini®, Molecular Devices).

2.9. DPPH radical-scavenging assay

Antioxidant activity was measured using a DPPH kit (Zantox, Iran) according to the manufacturer's protocol. DPPH solution (200 μM in methanol) was incubated in a dark place with increasing test concentrations (25, 50, 100, and 200 μg/mL) of 8-alkylmercaptocaffeine derivatives (compounds C1, C5, and C7) and CAF at 37 °C for 30 min. Next, the absorbance was read at 518 nm using an ELISA reader (Spectra Max Gemini®, Molecular Devices). At this time, the remaining DPPH is inversely proportional to the radical-scavenging activity of the compounds [29].

2.10. Measurement of malondialdehyde levels

Cells (1 × 10⁵ cell/mL) were seeded in a 6-well plate and exposed to 8-alkylmercaptocaffeine derivatives (C1, C5, and C7 equal to their IC₅₀ values) for 24 h. Malondialdehyde (MDA) level as a marker of lipid peroxidation was measured in cell pellets using the thiobarbituric acid reactive substance (TBARS) assay [30], according to the company's instruction (Teb Pazhouhan Razi, Tehran, IRAN). The absorption of the samples was read at 532 nm via a SpectraMax Gemini microtiter plate reader (Molecular Devices, Sunnyvale, CA). The protein concentration was assessed via the Bradford method [31], using a total protein assay kit (Teb Pazhouhan Razi, Tehran, IRAN) according to the manufacturer's protocol bovine serum albumin utilized as a standard. MDA

concentrations were expressed as nmol/mg of protein.

2.11. Molecular docking study

Since LeDock is a fast, simple, and accurate software for docking of small molecules in the computational study, thus, at first it was employed to start the Protein-ligand docking process (<http://lephar.com>), and also the HyperChem software was used for drawing the structure of all molecules (HyperChem(TM) Professional 7.51, Hypercube, Inc., 1115 NW 4th Street, Gainesville, Florida 32601, USA). The optimized ORCA software was applied to identify the geometry and energy of compounds at DFT, B3LYP/cc-pvdz level of theory [32]. The docking process was performed using chain A of the PDB structures of 1TBF [33], 6A3N [34] for PDE5 and PDE9, respectively. The homology model of PDE6 was constructed employing the chain A of PDB code 7JSN [35] as a template. The LePro module was examined to eliminate the crystallographic water molecules and cognate ligands from the molecule structure (<http://lephar.com>). Since it is a critical point to preserve the active site of the enzyme; thus, the docking parameters were arranged based on the center box of docking on the NE2 atom of Gln817 after superposition of all three structures on chain A of PDE5. The grid box was set to $10 \times 10 \times 10$ with a spacing value of 1.0 Å, and the number of binding poses was set to 200. Finally, an optimized conformation of the molecule having the least binding energy and great interacting residues was chosen.

2.11.1. Molecular dynamics simulations

Here, to examine the interactions of ligands with the active sites of PDE5, 6, and PDE9 and to observe the inhibitory performance of the ligands, compounds of the best docking pose were selected. After that, the molecular dynamic simulation technique was exploited to simulate the chosen compounds bound to each PDE for a period of 150 ns in explicit water (1.8 μs in aggregate). In this analysis, we consider a metalloprotein receptor whose mechanism is entirely zinc ion-dependent. The non-bonding model contains only the terms VDW and electrostatic between metal ions and ligands. [36] In this study, the CAF molecule was chosen as the control. Next, AmberTools package was employed as full Amber topology/coordinate files for all ligands [37]. Also, the VDW and bonded parameters of the different ligands were measured using the antechamber program of AmberTools by using the general amber force field (GAFF) [38]. At the same time, the protein was modeled by the AMBERff14SB force field [39]. To obtain the partial atomic charges, the RESP charge model was considered [40]. The TIP3P water model was introduced to solvate the compounds and ions added to the box to attain a neutral system. It should be said that the periodic boundary condition (PBC) was applied in three dimensions. All MD simulations were performed by a parallel version of SANDER in AmberTools 19 software package. It is worth noting that, before the MD simulation of protein–ligand complexes, the steepest descent algorithm was applied to minimize their energy. Additionally, a leap-frog algorithm was considered to integrate their motion [41]. In this process, to observe the effect of long-range electrostatic interactions of molecules, the Particle mesh Ewald (PME) method, similar to the previous research, was applied [42]. Also, to simulate H-bonds' limitations in this process, the LINKS algorithm was studied in both equilibration and production run [43]. The cutoff for nonbonded interactions was set to 12.0 nm. After the optimization of the system's energy, it was simulated for 20 ps in the canonical ensemble (NVT) and with a 1 ns time-step in the NPT ensemble. Also, two models, including Langevin dynamics [44] were studied to couple the temperature and pressure of the system using coupling constants of 0.1 and 0.5 ps, respectively.

2.11.2. Free energy calculations

The solvent and its interaction with biomolecules play pivotal roles in their structure, dynamics, and functions. However, lots of efforts have been put to develop several models to consider the solvent

contributions, especially in the biological system. Models of implicit solvent try for modeling the solute and solvent interactions in a mean-field fashion, saving the computational and sampling time. The performance of implicit models in many biological applications is significantly excellent and reproducible, though they are less precise. Principally, for evaluating the binding's free energy of small ligands to biological macromolecules, the molecular mechanics energies coupled with the Poisson–Boltzmann Surface Area (MM/PBSA) or Generalized Born Surface Area (MM/GBSA) as continuum solvation methods are known approaches. According to this research, in the Molecular Mechanics Poisson-Boltzmann Surface Area (MMPBSA) approach, we applied the PB-based solvent models to the protein–ligand binding interactions, primarily through combining with explicit solvent. As in the MMPBSA approach, it is allowed to address contributions from electrostatic and VDW interactions and changes in solvation to binding affinities [45].

To calculate the binding free energy (ΔG) of each small molecules as an inhibitor, we emphasized on equation (1):

$$\Delta G_{Bind} = G_{Com} - (G_{Rec} + G_{Lig}) = \Delta H - T\Delta S \approx \Delta E_{MM} + \Delta G_{Sol} - T\Delta S \quad (1)$$

In this equation, Com, Rec, and Lig subscripts are related to complex, receptor and ligand, and total binding energy presented by ΔG_{Bind} , introducing the differences free energy between G_{com} , and the sum of ($G_{Rec} + G_{Lig}$).

In the end-point binding free energy, including MM/GBSA and MM/PBSA, enthalpy is calculated, and to calculate entropy, one, should use the NMA and IE [46].

The free energy associated with equation (1) is the sum of four parts referred to equation (2):

$$\Delta G = (\Delta E_{MM}) + (\Delta G_{psolv}) + (\Delta G_{npsolv}) - T(\Delta S) \quad (2)$$

Where ΔE_{MM} in detail is:

$$\Delta E_{MM} = \Delta E_{Internal} + \Delta E_{Elec} + \Delta E_{VdW} \quad (3)$$

2.11.3. Energy decomposition and clustering analysis

The residue decomposition shows agreeable and disagreeable interaction data that is fruitful for lead improvement. In this study, for the residues with the most significant contributions to the inhibitor binding throughout the MD simulation course, the Water Swap residue-wise binding energy decompositions were assessed [47].

Clustering of MD frames is specifically helpful for molecular docking simulations. According to some criteria, MD frames located in the same group are similar to each other. Therefore, one could suppose that frames within the same cluster will behave similarly if a receptor in a cluster interacts agreeably with a specific ligand. The most traditional and known measure of similarity is the root mean square deviation (RMSD) values applied for partitioning MD trajectories gained by pairwise or matrix error distances [48].

2.12. Statistical analysis

SPSS v.23 software (SPSS Inc., Chicago, IL, USA) was used for data analysis. Results are expressed as mean \pm SE. Simple *t*-test and analysis of variance (ANOVA) were applied to determine the statistical significance between groups when appropriate. All assays were performed at least in triplicates, and *P*-value < 0.05 was considered significant.

3. Results

3.1. Cytotoxicity evaluation and analysis of drug combinations

The growth inhibitory effects of 8-alkylmercaptocaffeine derivatives were assessed against MCF7, KB, and A549 cancer cell lines. The cultivated cells were exposed to increasing concentrations of the compounds (25, 50, 100, and 200 μM), and cisplatin was used as a reference drug. As shown in Table 2, 8-alkylmercaptocaffeine derivatives showed a wide

Table 2

Cytotoxic activity of 8-alkylmercaptocaffeine derivatives determined by the MTT assay.

Compound	IC ₅₀ (μM) ^a		
	MCF-7	KB	A549
C1	49.7 ± 2.23	42.5 ± 2.12	97.6 ± 4.87
C2	>100	>100	>100
C3	83.73 ± 3.13	53.09 ± 3.76	>100
C4	47.94 ± 2.19	34.63 ± 2.87	>100
C5	79.65 ± 3.13	54.92 ± 3.17	92.38 ± 4.19
C6	>100	>100	>100
C7	47.66 ± 1.23	39.53 ± 2.09	65.8 ± 3.27
C8	>100	>100	>100
C9	>100	>100	>100
C10	44.76 ± 2.09	70.7 ± 3.98	>100
C11	40.92 ± 0.98	82.73 ± 2.69	>100
C12	>100	>100	>100
Cisplatin	6.58 ± 0.09	4.47 ± 0.07	6.76 ± 0.06

^a Values represent mean ± S.E.M.

range of cytotoxic activity in cancer cells; while having higher IC₅₀ values than cisplatin. Among them, compounds C1, C5, and C7 possessing propyl, heptyl, and 3-methyl-butyl moieties displayed better cytotoxicity against all three cell lines (IC₅₀ < 100 μM) and, therefore, selected for further assays. We then treated normal human cells with these three compounds within the given range. The IC₅₀ for compounds

C1, C5, and C7 in HUVEC cells were 114.97, 127.41, and 412.15 μM, respectively. This indicates that these derivatives exerted less inhibitory effects on non-malignant cells (higher IC₅₀ values). The cytotoxic activity of other compounds (C2, C3, C4, C6, C8, C9, C10, C11, and C12) was not desirable (IC₅₀ > 100 μM). Still, all these compounds exerted less toxicity than cisplatin alone.

Analysis of drug interactions revealed that the combination of cisplatin with compound C5 exerted synergistic anti-proliferative effects in MCF7 breast cancer cells (CI < 1 for all effective doses) (Fig. 1A). Contrastingly, in A549 lung cancer cells, a combination of these agents exhibited strong antagonism in different effect levels (CI > 1) (Fig. 1C). Fig. 1D shows the combination indices at different effective doses (EDs) for the combination of C1, C5, and C7 and cisplatin in the studied cell lines.

3.2. LDH-based cytotoxicity assay

Cytotoxic agents can damage the cell membrane and release cytosolic LDH in the media. Thus, the percentage of LDH leakage is an indicator of cell membrane disruption due to necrosis or late-stage apoptosis. As depicted in Fig. 2A, the percentage of LDH leakage in MCF7, KB, and A549 cells remained insignificant and at low levels (<20%), in comparison with the level of the untreated cells (P < 0.05). This shows that 8-alkylmercaptocaffeine derivatives (C1, C5, and C7) only induced minimal necrotic damage to these cells and had negligible

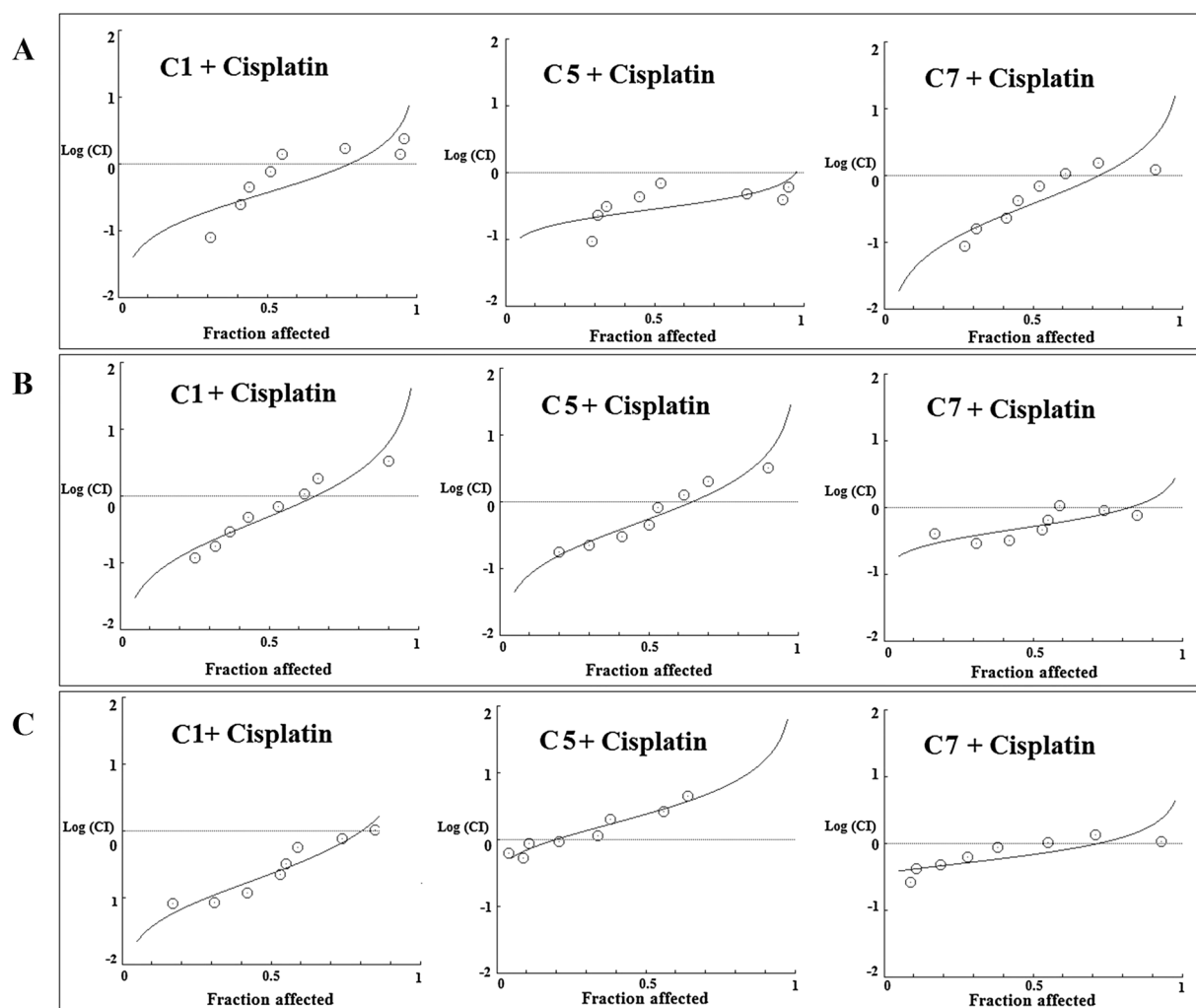


Fig. 1. Combination index (CI) plot (Log CI) for the combination of three 8-alkylmercaptocaffeine derivatives (C1, C5, and C7) and cisplatin in MCF-7 (A), KB (B), and A549 (C) cancer cells. Different effective doses (EDs) of the combinations in the studied cell lines (D).

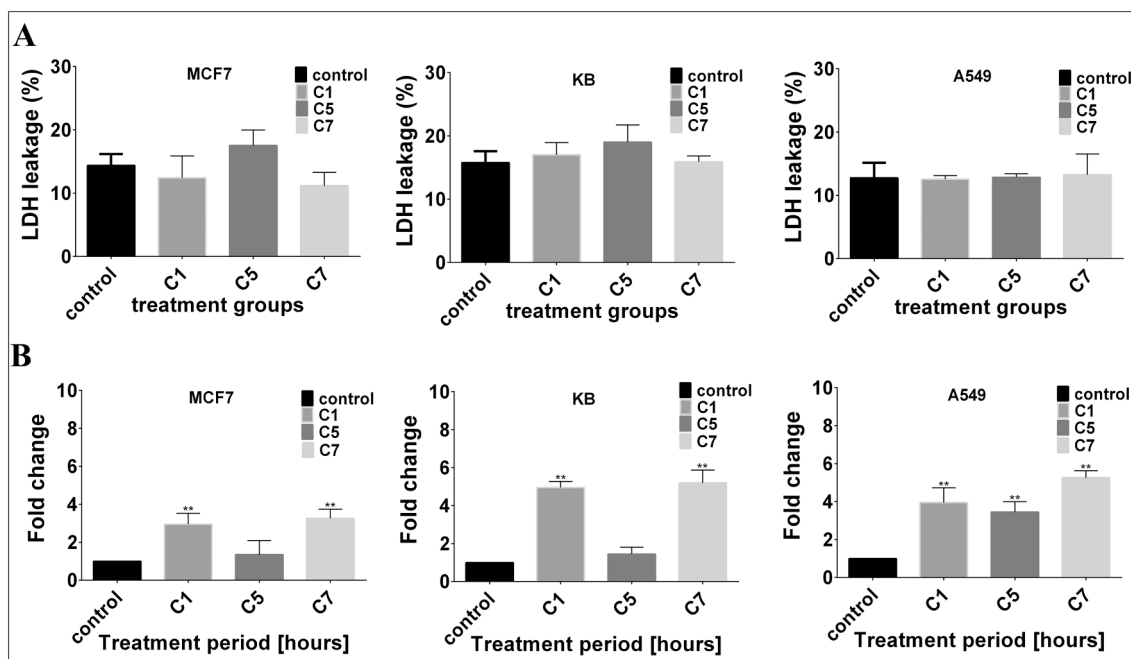


Fig. 2. The percentage of LDH leakage from untreated cancer cells and cells treated with three 8-alkylmercaptocaffeine derivatives (C1, C5, and C7) for 24 h (A). Effects of C1, C5, and C7 on caspase-3 activity in MCF7, KB, and A549 cell lines following 24 h of exposure (B). Effect of three 8-alkylmercaptocaffeine derivatives (C1, C5, and C7) on cGMP levels in MCF-7, KB, and A549 cells (C). ** $P < 0.05$ compared to untreated cells.

effects on the release of intracellular LDH.

3.3. Caspase-3 activation

As an essential executioner caspase, caspase-3 is needed for nuclear changes associated with apoptotic cell death. Treatment with 8-alkylmercaptocaffeine derivatives showed a significant increase in caspase-

3 activity in MCF7 (treated with C1 and C7), KB (treated with C1 and C7), and A549 (treated with C1, C5, and C7) cell lines ($P < 0.05$ compared with adjusted untreated cells). As shown in Fig. 2B, the role of C5 in caspase-3 activation differs between cell lines. However, we suggest that cell death induced by C1 and C7 was mediated by apoptosis rather than necrosis.

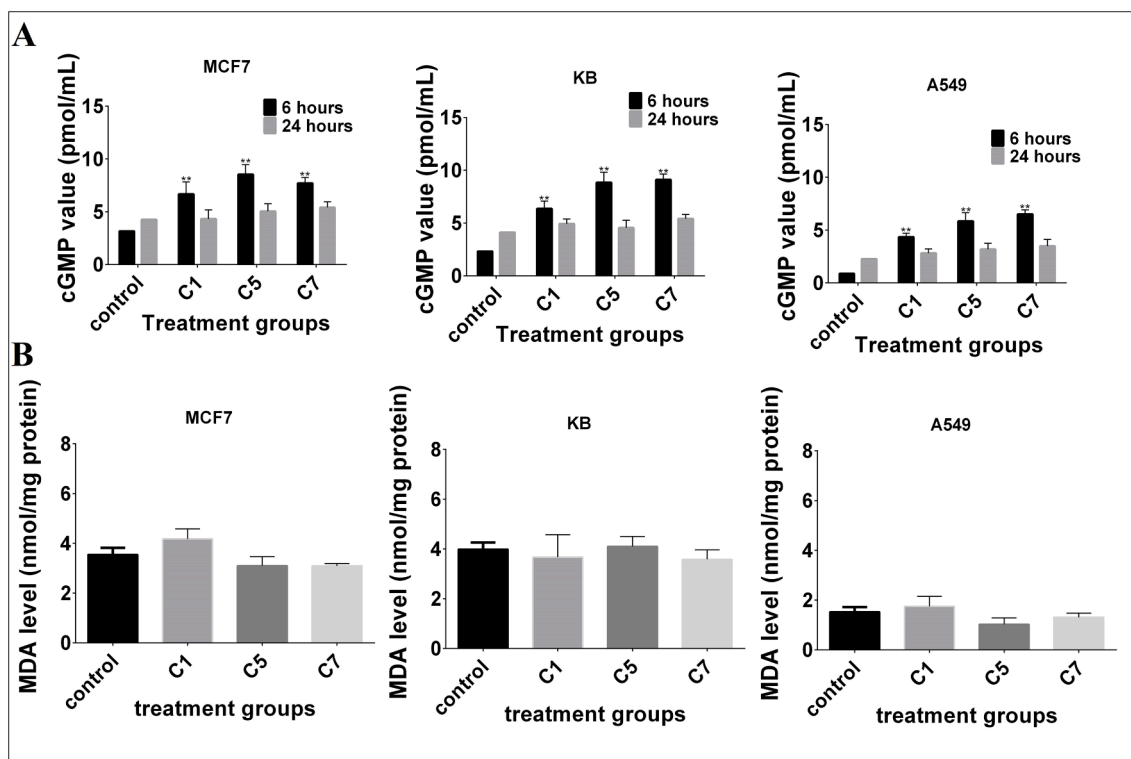


Fig. 3. Assessment of lipid peroxidation within 24 h in MCF7, KB, and A549 cells after treatment with three 8-alkylmercaptocaffeine derivatives (C1, C5, and C7).

3.4. cGMP levels

Hydrolysis of cGMP is mediated by phosphodiesterases (PDEs); hence, PDE inhibitors increase cGMP levels. Effects of selected derivatives of 8-alkylmercaptocaffeine on intracellular cGMP in cancer cells were assessed. Our results demonstrated that C1, C5, and C7 significantly improved cGMP levels at 6 h in MCF7, KB, and A549 cells, compared to those of untreated cells ($P < 0.05$) (Fig. 2C). However, cGMP levels returned to baseline after 24 h. These findings suggest that PDE inhibition, specifically by 8-alkylmercaptocaffeine derivatives bearing heptyl and 3-methyl-butyl moieties, augmented cGMP values in cell lines derived from breast, lung, and oral tumors.

3.5. Antioxidant properties of 8-alkylmercaptocaffeine

A 24 h treatment of MCF7, KB, and A549 cells with selected compounds (C1, C5, and C7) did not lead to any significant change in the cellular concentration of MDA, suggesting that these derivatives were not able to attenuate lipid peroxidation and exerted no ameliorative effects ($P > 0.05$) (Fig. 3A). Fig. 4 shows the concentration-dependent antioxidant capacity of these compounds. Compared to CAF as the reference compound, only C5 significantly scavenged the DPPH and increased with increasing concentrations ($P < 0.05$).

3.6. Molecular docking and molecular dynamics analysis

A comparative study has been done to find the binding modes of small molecules in the active site of PDE5A using varieties of docking programs [49]. Validation of docking was performed in terms of reproducibility of native ligand (Sildenafil) in the X-ray crystal structure (PDB ID: 1TBF). The re-docking results have been shown in Fig. 5A. As shown, there is a good match between the results of LeDock and the crystallographic structure. Fig. 5B shows the main interactions of Sildenafil, which include a bidentate hydrogen bond (H-Bond) between the nitrogen atom of pyrazolo[4,3-D] pyrimidine moiety with Gln817.

The synthesized structures (C1, C5, and C7), as well as CAF and Sildenafil, were docked into the three PDEs receptors (Table 3). As shown, CAF exhibits the least binding energy of -4.22 , -2.45 , and -4.71 kcal/mol against PDE5, PDE6, and PDE9, respectively, while the synthesized compound C5 showed the maximum binding energy of -6.39 , -3.49 , and -6.17 kcal/mol in respect to the aforementioned receptors. It is evident from Table 3 that the C5 is a more potent compound towards the PDE5 based on the docking results.

The best docking poses of the compounds above with PDE5A and PDE9A were depicted in Fig. 6. Docking poses for PDE6A were not depicted in the figure because of lacking permeant interaction of ligand

in the active site of the protein. The pattern of forming an H-bond between the nitrogen atom of pyrazolo[4,3-D] pyrimidine moiety of Sildenafil and Gln817 was observed in all ligands except C1 towards PDE5A. Moreover, the oxygen atom in this moiety forms H-bond with the hydroxyl group of Tyr612 in PDE5A (Fig. 6). The hydrophobic pocket formed by Phe820, Val782, Leu804, and Phe786 helps the alkyl chain of synthesized ligands to reside well in the active site of this enzyme. In all ligands (except for C1), Phe820 is responsible for forming a π - π stacking with the aromatic ring of pyrazolo[4,3-D] pyrimidine moiety in the case of PDE5A. The docking study reveals the different patterns in residing the synthesized ligand towards PDE9A. Fig. 6 illustrates that the docking poses of ligands, as contrasted with PDE5A pattern, showing oxygen atom in pyrazolo[4,3-D] pyrimidine involved in interaction with Gln453. It is believed that the Phe456 in PDE9A helps ligand to accommodate in the active site of the enzyme by forming π - π stacking with the aromatic ring of pyrazolo[4,3-D] pyrimidine moiety.

Root mean square deviation (RMSD) of C α atoms of PDE5, 6 and 9 backbone were monitored throughout 150 ns MD simulation (Fig. 7A-C). RMSD analysis showed the differences in the backbone motion of each enzyme in the presence of the ligands. The CA atoms fluctuation in PDE5 (Fig. 7A) and PDE9 (Fig. 7C) follows the same pattern showing the fluctuation about 1 and 2 rather than 4 order of magnitude in PDE6 (Fig. 7B). More restriction in motions occurs when these ligands are bound to PDE5 and 9, according to RMSD plots.

The root mean square fluctuation (RMSF), as the fluctuation of every single atom about its average position, was calculated for three PDEs in the presence of ligands and depicted in Fig. 8A-C. It can be witnessed from Fig. 8A that the C5 and C8 compounds changed the fluctuations in residue ranges 650–680 and 730–760 in PDE5A. In the case of PDE9A enzyme, huge fluctuations occurred in residue range 425–450, as depicted in Fig. 8C.

Conformational clustering was performed on the molecular dynamic trajectory of the aforementioned ligand–protein complexes to intelligently select representative conformations for further analysis. Clustering was performed employing k-means algorithms by using RMSD of residues with sieving frame by 10. However, we considered the center structures of most populated and hence more stable clusters as representatives of binding mode conformations (Fig. 9A-C). Analysis of PDEs active site reveals four key interactions that affect cyclic nucleotide selectivity and catalysis: (1) metal-binding; (2) coordination to the phosphate group; (3) hydrophobic “clamp” that affords affinity; and (4) hydrogen-bonding network that determines nucleotide selectivity [33].

As shown in Fig. 9, there are two important factors, including i) the presence of hydrogen bond between the nitrogen atom in the pyrazolo [4,3-D] pyrimidine group with Gln817 in PDE5A (Fig. 9a), the hydrogen bond between oxygen atom in the pyrazolo[4,3-D] pyrimidine group with Gln773 in PDE6A (Fig. 9b) and hydrogen bond between oxygen atom in the pyrazolo[4,3-D] pyrimidine group with Gln453 in PDE9A (Fig. 9c); ii) creation of a hydrophobic cavity, which results in the better stability of the alkyl group in the active site. However, compound C1, despite having the latter factor, shows less stability due to the lack of a strong H-bond (see the next section) with Gln817 and due to the rotation in the active site during the MD simulation course. (Fig. 9A).

3.7. Hydrogen bond analysis

In order to determine the stability of hydrogen bonds between CAF, C1, C5, and C7 with PDE5A, PDE6A, and PDE9A, MD analysis of ligand-enzyme complex stability were performed during the 150 ns of trajectory period. Hydrogen bond profiles between the selected ligands and the enzyme were calculated using the H-bond utility of AmberTools19. The threshold for H-bond forming was 3.0 Å with an angle of 135°. The results of the analysis have been shown in Table 4. The percent of occupancy shows the number of frames in which the particular H-bond has been monitored out of all processed frames. The H-bonding network, as has been described in the study of Zhang and coworkers [33], plays a

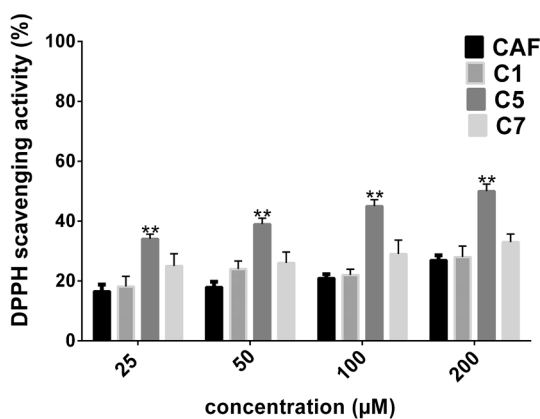


Fig. 4. Concentration-dependent DPPH radical scavenging activity of 8-alkylmercaptocaffeine derivatives (C1, C5, and C7). ** $P < 0.05$ compared to CAF as the reference compound.

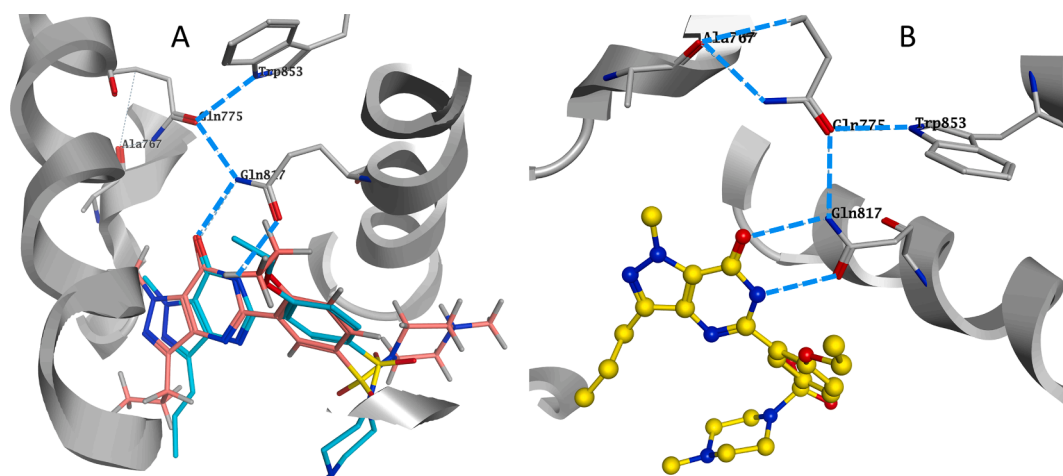


Fig. 5. (A) Redocking and superposition of Sildenafil in native structure (PDB ID: 1TBF). (B) Hydrogen Bond network of Sildenafil in the active site of PDE5A. Sildenafil starts to be recognized by Gln817 through bidentate H-bond. The orientation of the Gln817 side chain is anchored by its H-bond interaction with Gln775. The orientation of Gln775 side chain is in turn anchored by the H-bond between Ne in Gln775 and the carbonyl oxygen in Ala767 and the H-bond between Oe of Gln775 and the Ne of Tyr853.

Table 3
2D representation and docking results (in kcal/mol) of selected ligands.

Selected Ligands	Chemical Structure	Docking Result		
		PDE5	PDE6	PDE9
CAF		-4.22	-2.45	-4.71
C1		-5.42	-3.01	-5.20
C5		-6.39	-3.49	-6.17
C7		-5.64	-3.37	-5.70
Sildenafil		-8.57	-	-

crucial role in GMP recognition by PED5A and the other PDEs. Therefore, those inhibitors which disrupting this H-bonding network are supposed to have a better inhibitory effect. The analysis disclosed that the stable hydrogen bond between Gln775 in PDE5A and Gln453 in PDE9A is the key residue in forming the H-bonding network. One of the oxygen atoms in the pyrazolo[4,3-D] pyrimidine group has a remarkable impact on the order of inhibition activities of the C5 and C7 (with occupancy of 6.21% and 3.09%, respectively). At the same time, the lack of this interaction during the MD simulation can be attributed to the low binding affinity of CAF and C1 in PDE5A (Table 4). In PDE9A, inhibitors possessing the key residues His252 and Met365 are supposed to have remarkable inhibition effects on this enzyme [50]. However, according to table 4, the C5 compound, by engaging itself with His252, showed better inhibition.

The hydrogen bond analysis can also promise the emergence of another pharmacophore in the desired compounds. One can define this pharmacophore as a hydrogen bond, as it is formed by the hydroxyl

group of Tyr612 with corresponding atoms in C1, C5, C7, and CAF in PDE5A.

3.8. Binding free energy and energy decomposition analysis

The binding affinity of chosen ligands was studied based on binding free energy estimated using MM-PB/GBSA method. 1000 snapshots of the MD trajectory were taken to measure the MM-GB / PBSA binding energy. Based on the extensive tests and the better agreement with the PB treatment in calculating the electrostatic part of the solvation energy, the modified GB model was developed by Onufriev and Case (igb = 5 termed as GB^{OBCL}) used in the GB calculations. The solute dielectric constant was set to 1 [51]. The solcon parameter was set to 0.15 M for reconciliation between PB and GB solvation energies, as described in S. Srinivasan's work [52]. Table 5 provides the details of contribution terms in the binding free energies of the inhibitors against PDE5, 6, and 9A according to the definitions in equations (1)–(4). As can be inferred from Table 5, the free energy order and thus the inhibition efficiency of the ligands against PDE5A is as follows: C5 > C7 > C1 > CAF. Table 5 also has revealed that the synthesized compounds are supposed to have the same potency order against PDE6A, with C5 is the most potent inhibitor in this category. However, the scenario for PDE9A is different in terms of the binding free energy of listed ligands against this enzyme. According to table 5, C7 compound is the most potent inhibitor against PDE9A, followed by C1 and C5. The MMPBSA calculation can provide extra information to determine the relative contribution of each residue, as decomposition analysis, to the binding free energy of PDE5A/ligand complexes. The results have been shown in Fig. 10.

4. Discussion

Since the discovery of 6-mercaptopurine (6-MP) as a chemotherapeutic agent [53,54], many attempts have been made on synthesizing a variety of methylxanthines based on the mercapto moiety into their scaffolds.

In this study, we found more desirable cytotoxic effects for 8-alkylmercaptocaffeine derivatives having propyl, heptyl, and 3-methylbutyl substitutes in cancer cells derived from breast, lung, and oral human tissues. Our new alkylmercaptocaffeine precursors bearing heptyl moiety also enhanced the cytotoxic effects of cisplatin in MCF7 breast cancer cells. It has been established that xanthine derivatives [55] or CAF itself [56] could synergistically sensitize cancer cells to cisplatin. Besides, it appears that these three selected compounds, C1, C5, and C7,

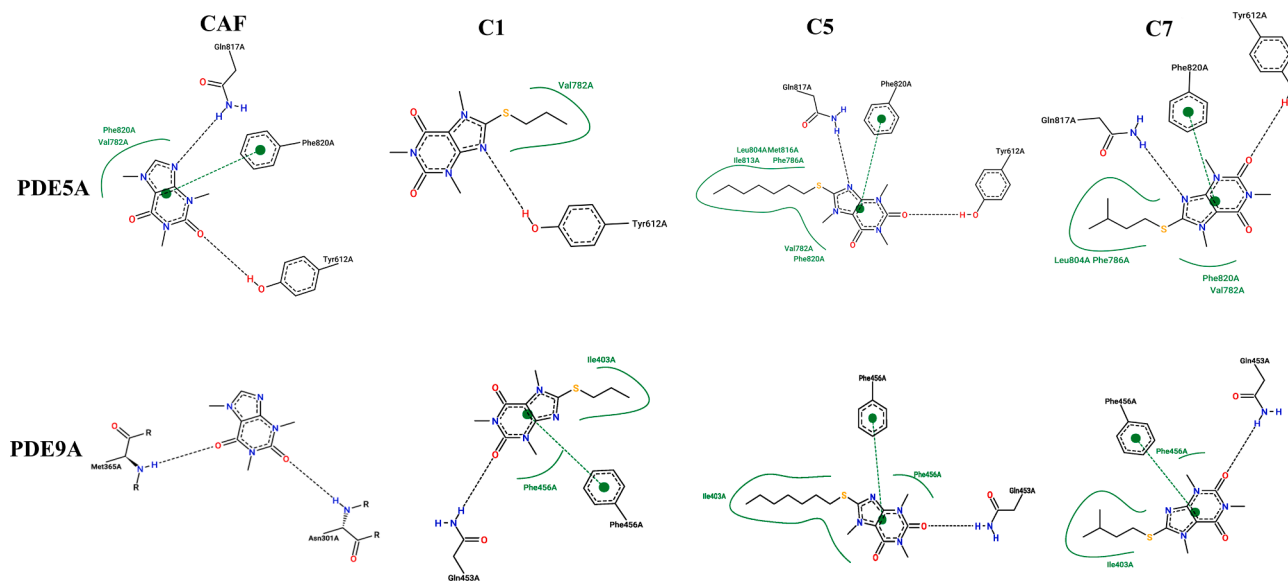
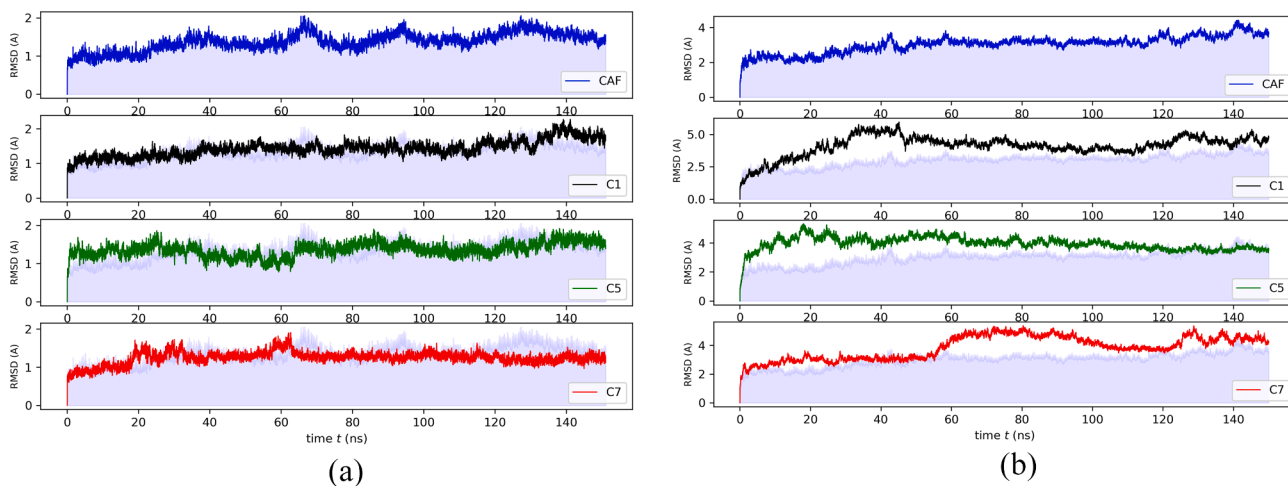
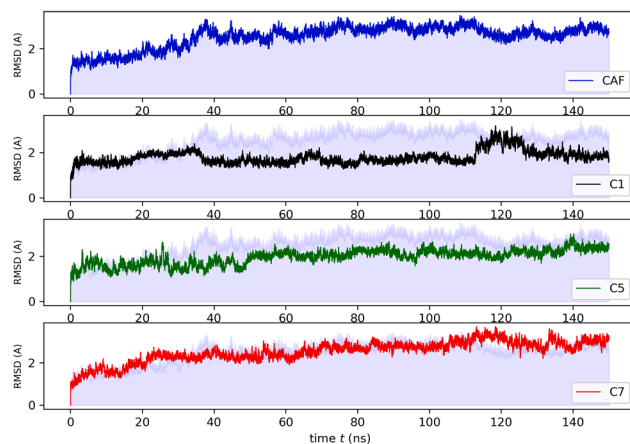


Fig. 6. Binding modes of the ligands in 2D representation obtained from docking simulation. Hydrogen bonds are depicted as a straight dashed line, while the hydrophobic interactions are shown as curved line.



(a)

(b)



(c)

Fig. 7. RMSD plots of CA atoms of (A) PDE5A, (B) PDE6A and (C) PDE9A bound to the 3 selected ligands as well as reference compound (CAF).

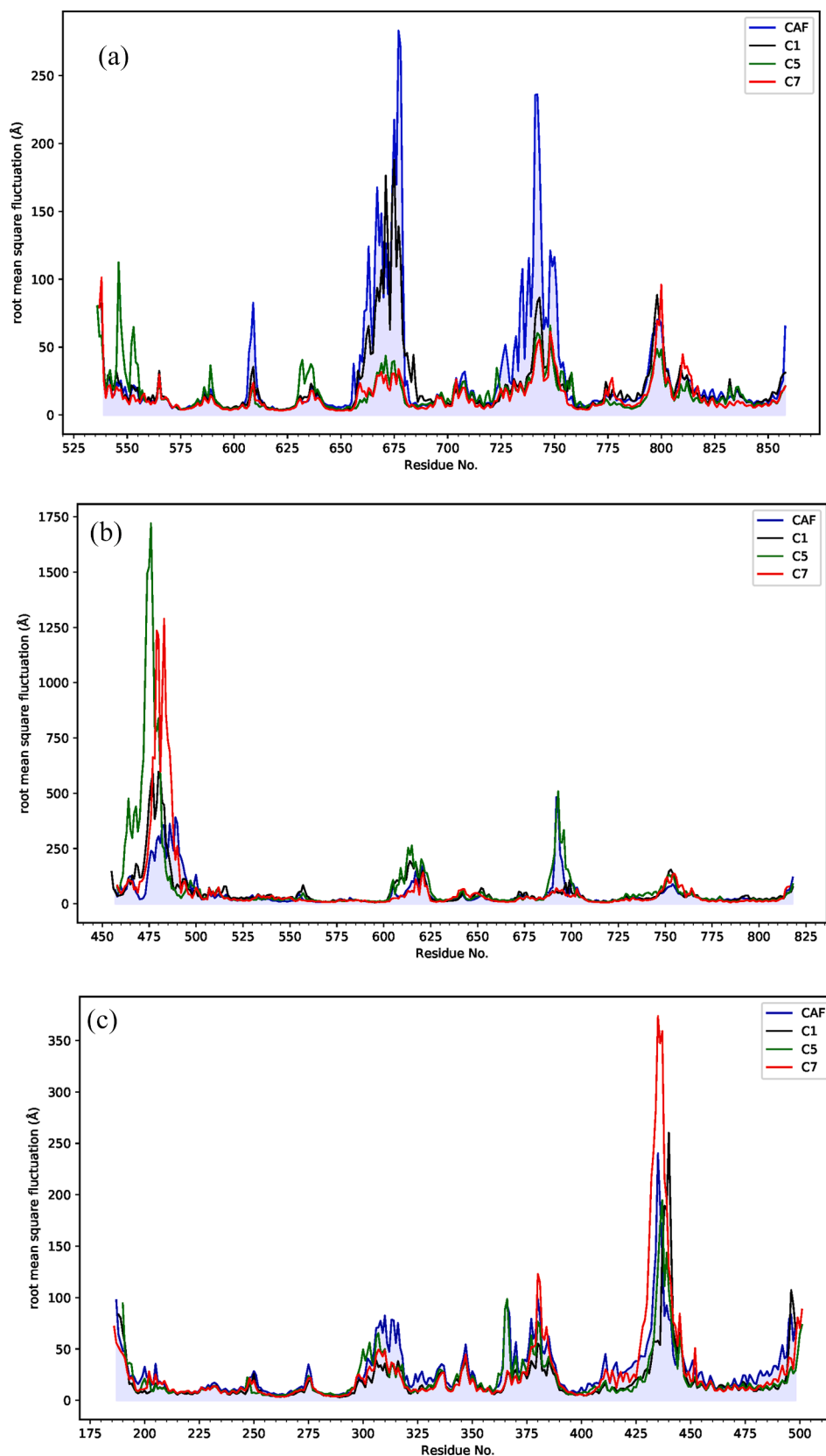


Fig. 8. Root-mean-square fluctuation (RMSF) per residue of C1 (Black), C5 (Green), C7 (Red), and CAF (Blue) bound to (A) PDE5A, (B) PDE6A and (C) PDE9A. (For interpretation of the references to colour in this figure legend, the reader is referred to the web version of this article.)

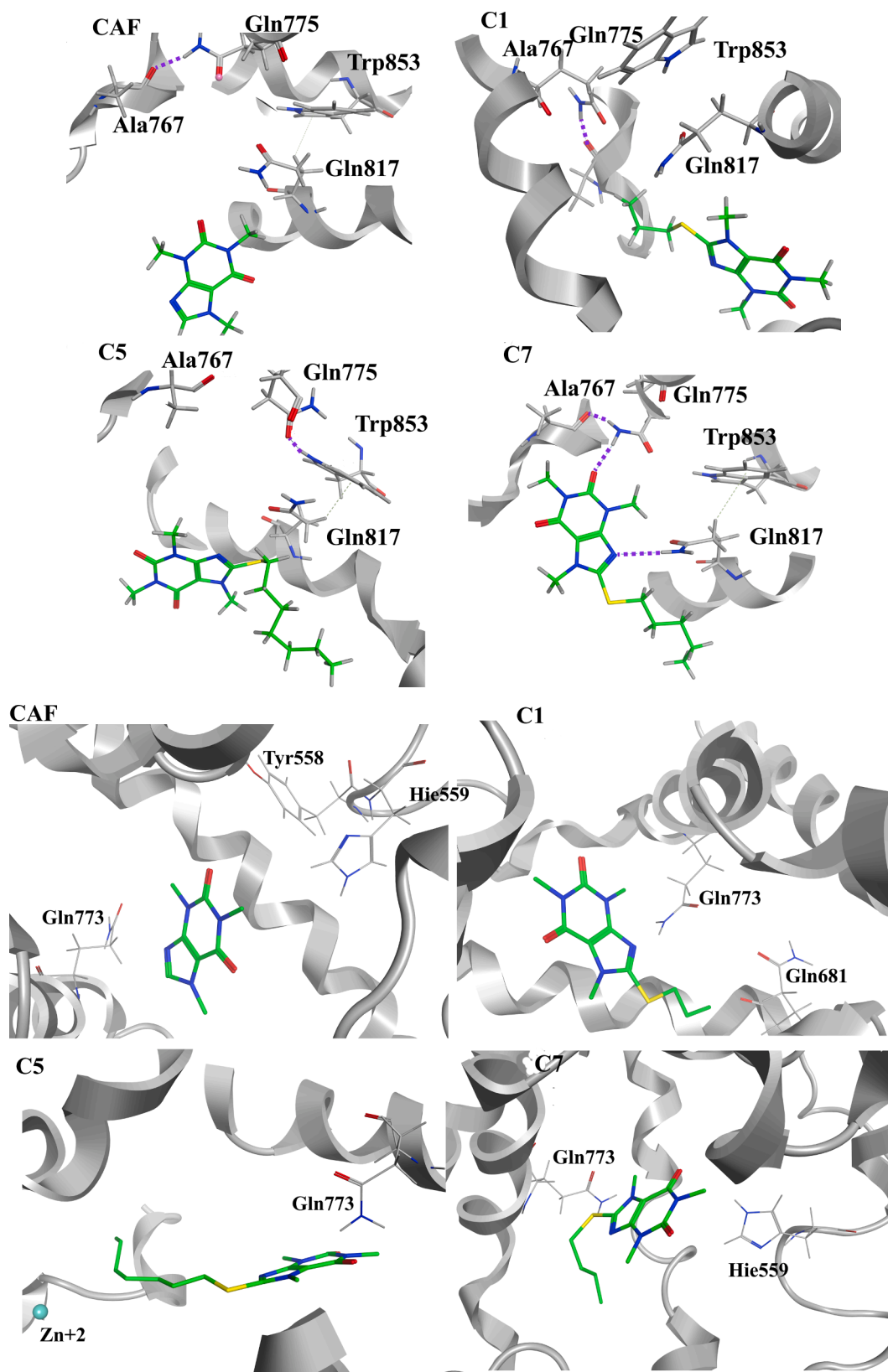


Fig. 9. Binding mode of CAF, C1, C5, and C7 as a result of clustering analysis shown as green thick stick models with the active site of (A) PDE5A, (B) PDE6A and (C) PDE9A.α helix are shown as helix representation. Important residues interactions involved in ligand binding are shown as purple. (For interpretation of the references to colour in this figure legend, the reader is referred to the web version of this article.)

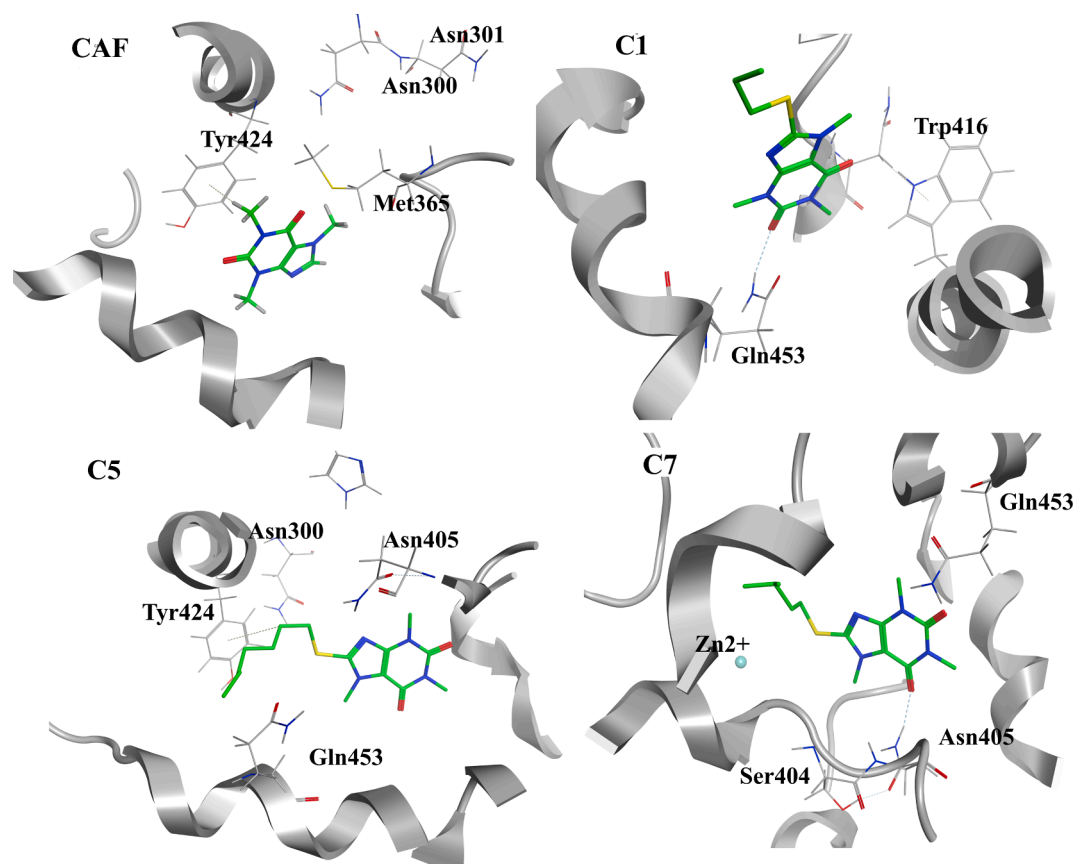


Fig. 9. (continued).

Table 4

Hydrogen bond analysis for all ligands as well as CAF as a control compound in this study.

Hydrogen Bonds								
	PDE5		-	PDE6		-	PDE9	
	Acceptor	Donor		Acceptor	Donor		Acceptor	Donor
CAF (control)	CAF@O2	GLN817@NE2 (6.12)	CAF@O11	GLN773@NE2 (0.043)	CAF@O11	ASN301@N (0.022)		
	CAF@N9	GLN817@NE2 (1.72)	CAF@N1	GLN773@NE2 (0.011)	CAF@O11	TYR424@OH (0.012)		
	CAF@O6	GLN817@NE2 (0.39)	CAF@O10	GLN773@NE2 (0.007)	CAF@O10	ASN300@ND2 (0.010)		
	CAF@O2	TYR612@OH (0.16)	CAF@N1	HIE559@OH (0.006)	CAF@O10	MET365@N (0.007)		
C1	C1@N18	TYR612@OH (0.57)	C1@N11	GLN773@NE2 (0.008)	C1@O7	GLN453@NE2 (0.63)		
	C1@O10	GLN817@NE2 (0.43)	C1@O3	GLN731@NE2 (0.006)	C1@O3	TRP416@NE1 (0.29)		
	C1@O9	TYR612@OH (0.07)	C1@O7	ASN607@ND2 (0.001)	C1@O3	ASN405@ND2 (0.03)		
	C5@O9	GLN775@NE2 (6.21)	C5@O3	GLN773@NE2 (0.024)	C5@O9	ASN405@N (0.096)		
C5	C5@N22	GLN817@NE2 (0.76)	C5@O3	GLN773@NE2 (0.003)	C5@N22	GLN453@NE2 (0.091)		
	C5@O10	TYR612@OH (0.69)	C5@O7	GLN773@NE1 (0.001)	C5@O10	HIE252@NE2 (0.038)		
	C5@O9	TYR612@OH (0.62)						
C7	C8@O9	GLN775@NE2 (16.48)	C8@O3	GLN773@NE2 (0.08)	C8@O3	ASN405@ND2 (0.73)		
	C8@O9	GLN817@NE2 (3.09)	C8@O7	GLN773@NE2 (0.04)	C8@O7	GLN453@NE2 (0.29)		
	C8@N21	GLN817@NE2 (2.57)	C8@O7	HIE559@OH (0.002)	C8@O3	SER404@OG (0.0)		
	C8@O10	TYR612@OH (0.97)			C8@O7	GLN453@NE2 (0.0)		
	C8@O9	TYR612@OH (0.10)						

CAF: Caffeine.

The occupancy percentage are represented in parentheses.

mediate their cell-death-inducing effects through caspase-3 dependent apoptosis rather than necrosis. However, performing more assays such as flow cytometry and DAPI staining are needed to detect apoptosis. Still, our results agreed with the findings of Liu et al., suggesting that CAF induces sustained apoptosis in HepG2 liver cancer cells through activation of the caspase-3/caspase-9 signaling pathway [57]. Later, we found that the three selected derivatives of 8-alkylmercaptocaffeine prompt cGMP levels in MCF7, KB, and A549 cells, suggesting the role of synthesized compounds for effective inhibition of PDEs, and

therefore, regulation of cGMP hydrolysis in these cells. From the standpoint of structural activity relationship (SAR), it is a proven fact that the site of alkylation almost determines the biological activity of the corresponding methylxanthine. The C(8) alkylation/substitution of CAF has often provided a large series of analogues with potential antirhinis or antagonistic property for adenosine receptors as well as PDE. Hence, many efforts have been put into synthesizing manifold 8-mercaptocaffeine derivatives which have grabbed much attention since their significant pharmaceutical profiles. Mostert et. el synthesized a series of 8-

Table 5

Binding free energy and its components obtained by MM-PB/GBSA calculation for all ligands.

			CAF	C1	C5	C8		
PDE5	MMPBSA	ΔE_{VDW}	-24.04	-33.45	-48.44	-34.19		
		ΔE_{elec}	-0.71	-0.52	-0.44	-0.39		
		ΔE_{PB}	3.05	4.07	4.76	3.39		
		ΔE_{NP}	-16.54	-23.27	-32.61	-23.25		
		ΔG_{solv}	14.88	20.53	26.38	20.45		
		ΔG_{gas}	-24.75	-33.96	-48.89	-34.59		
		$-T\Delta S$	15.99 ± 0.49	20.61 ± 1.20	26.04 ± 1.01	20.52 ± 0.97		
		ΔG_{Bind}	-9.86 ± 2.13	-13.43 ± 2.73	-22.50 ± 3.22	-14.13 ± 2.58		
		MMGBSA	ΔE_{VDW}	-24.04	-33.45	-48.44	-34.19	
			ΔE_{elec}	-2.85	-2.06	-1.77	-1.57	
	ΔE_{GB}		14.78	17.74	18.12	14.72		
	ΔE_{Surf}		-2.64	-3.83	-5.77	-3.76		
	ΔG_{solv}		12.14	13.91	12.35	10.96		
	ΔG_{gas}		-26.89	-35.51	-50.22	-35.77		
	ΔG_{Bind}		-14.75 ± 1.78	-21.60 ± 2.20	-37.87 ± 2.81	-24.81 ± 2.61		
	PDE6		MMPBSA	ΔE_{VDW}	-24.11	-36.44	-39.80	-38.94
				ΔE_{elec}	-0.63	-0.69	-1.83	-1.32
				ΔE_{PB}	3.08	4.08	6.35	4.70
		ΔE_{NP}		-16.51	-24.71	-29.08	-25.84	
		ΔG_{solv}		15.57	20.81	28.04	24.44	
ΔG_{gas}		-24.74	-37.13	-41.64	-40.26			
MMGBSA		ΔG_{Bind}	-9.17 ± 2.24	-16.31 ± 2.44	-13.59 ± 3.93	-15.82 ± 3.04		
		ΔE_{VDW}	-24.11	-36.44	-39.80	-38.94		
		ΔE_{elec}	-2.52	-2.76	-7.35	-5.29		
		ΔE_{GB}	13.88	18.67	24.26	21.43		
	ΔE_{Surf}	-2.61	-4.22	-4.94	-4.38			
PDE9	MMPBSA	ΔG_{solv}	11.26	14.44	19.32	17.05		
		ΔG_{gas}	-26.63	-39.20	-47.16	-44.23		
		ΔG_{Bind}	-15.37 ± 2.15	-24.76 ± 2.11	-27.83 ± 3.40	-27.18 ± 3.28		
		MMGBSA	ΔE_{VDW}	-25.37	-36.27	-39.11	-44.68	
			ΔE_{elec}	-0.37	-2.34	-1.41	-2.44	
	ΔE_{PB}		3.14	6.61	17.50	10.39		
	ΔE_{NP}		-15.95	-24.68	-27.07	-28.44		
	ΔG_{solv}		15.21	25.43	40.11	32.42		
	ΔG_{gas}	-25.75	-38.62	-40.52	-47.13			
	ΔG_{Bind}	-10.54 ± 2.72	-13.18 ± 2.70	-0.41 ± 8.57	-14.71 ± 3.58			
MMGBSA	ΔE_{VDW}	-25.37	-36.27	-39.11	-44.68			
	ΔE_{elec}	-1.50	-9.37	-5.64	-9.79			
	ΔE_{GB}	13.27	25.22	32.25	32.76			
	ΔE_{Surf}	-2.59	-4.41	-4.71	-5.14			
	ΔG_{solv}	10.67	20.81	27.53	27.61			
ΔG_{gas}	-26.88	-45.65	-44.76	-54.48				
ΔG_{Bind}	-16.20 ± 2.74	-24.83 ± 3.02	-17.22 ± 6.37	-26.87 ± 3.09				

[(phenylethyl)sulfanyl] CAF analogues and evaluated them as inhibitors of human MAO-A and -B. Among the synthesized compounds, 8-[(phenylethyl)sulfanyl] CAF (IC₅₀ = 0.223 μM) showed potent inhibitor of the type MAO-B isoform [58]. A year after, Rivara et. al, decided to assess the likelihood of generating new dual A2A antagonists/MAO-B inhibitors with potential biological activity at the two targets. To select a suitable scaffold, they designed new compounds based on caffeinyl core. They observed that in position 8 of the 9-deazaxanthine scaffold, either a benzyloxy or a phenylalkynyl substituent of CAF led to compounds with noticeable MAO-B inhibitory potencies [59]. Krutovskikh et. al synthesized 8-β-dialkylaminoethylmercaptocaffeine derivatives with radioprotective property [60]. Furthermore, caffeine-8-thioglycolic acid analogues were designed by Mitkov and coworkers with brain antihypoxic activity [61]. Here, our aims are to discover new inhibitors of the PDE enzymes, particularly the PDE 6 and 9 isoform. This study is a continuation of an our continual interest on synthesis of new methylxanthine derivatives [62]. In an effort to investigate the anticancer effects of PDE

inhibitors, a series of 8-alkylmercaptocaffeine derivatives was synthesized and evaluated for their biological activities. Supplementary figure shows various modifications (alkylation or substitution) of methylxanthines lead to diverse pharmaceutical properties. For the purpose of this study 8-alkylmercaptocaffeine homologues containing different alkyl group substituents on the C8 were considered. The results showed that only aliphatic substitutions at C8 bear cytotoxicity against A549 cell line. These compounds also exhibited good cytotoxicity against KB cells while C10 and C11 with aromatic substitution at C8 showed the highest activity against MCF7 cells. We found that although some of 8-alkylmercaptocaffeine derivatives showed much better cytotoxic effects against cancer cells, these compounds could trigger cell death through caspase-3 and vGMP-dependent mechanisms, besides being potent inhibitors against PDE 5A, 6A, and 9A.

On the other hand, PDE5 inhibitors have been introduced as potent antioxidants, which enhance the enzymatic antioxidants' system capacity and restore redox imbalance [63]. In contrast, it has been shown that CAF, along with its catabolite products, exhibits both antioxidant and prooxidant properties [64]. Our synthesized compounds, however, did not show ameliorative effects on lipid peroxidation, and therefore might not exert antioxidant activity. Furthermore, the antioxidant capacity of selected derivatives of 8-alkylmercaptocaffeine was analyzed via DPPH assay. We found higher antioxidant activity than CAF for only one compound (C5).

Based on computational studies, it seems that VDW, Non-polar interaction strongly favors the stability of C5, C7, and C1 in the active site of the enzyme. The favorable interactions of VDW can be attributed to the alkyl chain interactions with residues in the active site of the protein. According to the results that have been shown in Fig. 10, decomposition analysis reveals that the Phe820 has a considerable contribution to the binding of four ligands, specifically for CAF and C7 compounds. This residue favors accommodation of ligands by van der Waals interaction with the alkyl chain of the ligands. Another key interaction that affects cyclic nucleotide selectivity and catalysis of PDE5A is the metal binding. Energy decomposition analysis shows the contribution of zinc ions in the binding of synthesized ligands and CAF. It can be inferred that the zinc ion cooperates in binding by favoring the long-range electrostatic energy interaction with ligands, which especially has a dominant role in the binding of C5 and C7.

It should be noted that, unlike electrostatic interaction, the polar solvation energy disfavors the binding of the ligands. Detecting the residues involved in the hydrogen-bonding network, which has a massive contribution to the nucleotide selectivity of PDE5A, and their decomposition energy, gives us a perspective of the efficiency of the ligands above. It is evident from Fig. 10, residues around the Ala767 like Asp764, Leu764, Leu765, and, Ile768 show an insignificant impact on the binding energy of the ligands. Likewise, Met816 and Gly819 in the vicinity of Gln817 exert their non-dominant positive effects by VDW interaction, although the polar solvation interaction of these residues may neutralize their positive impact.

THE human *PDE5A* gene encodes three PDE5 isoforms from two alternative promoters, including *PDE5A1*, *PDE5A2*, and *PDE5A3*. The *PDE5* gene is highly expressed in several cancer-associated tissues, such as breast tumors [65]. Lately, many studies have concentrated on using PDE inhibitors as a novel therapeutic opportunity for multiple cancers. In this regard, attempts have been made to utilize PDE inhibitors alone and in combination with traditional chemotherapeutic agents to kill cancer cells more effectively [66]. Much recently, Piazza and coworkers demonstrated how PDE5 inhibition triggers the cGMP/PKG signaling pathway to suppress Wnt/β-catenin transcription and proliferation of cancer cells [67]. In the present study, we have demonstrated that 8-alkylmercaptocaffeine derivatives with propyl, heptyl, and 3-methylbutyl moieties have favorable cytotoxic properties in different cancer cells, possibly through induction of cell death via cGMP signaling. These findings agreed with previous studies using cancer cells, reporting that cGMP plays a pivotal role in suppressing cell growth and induction of

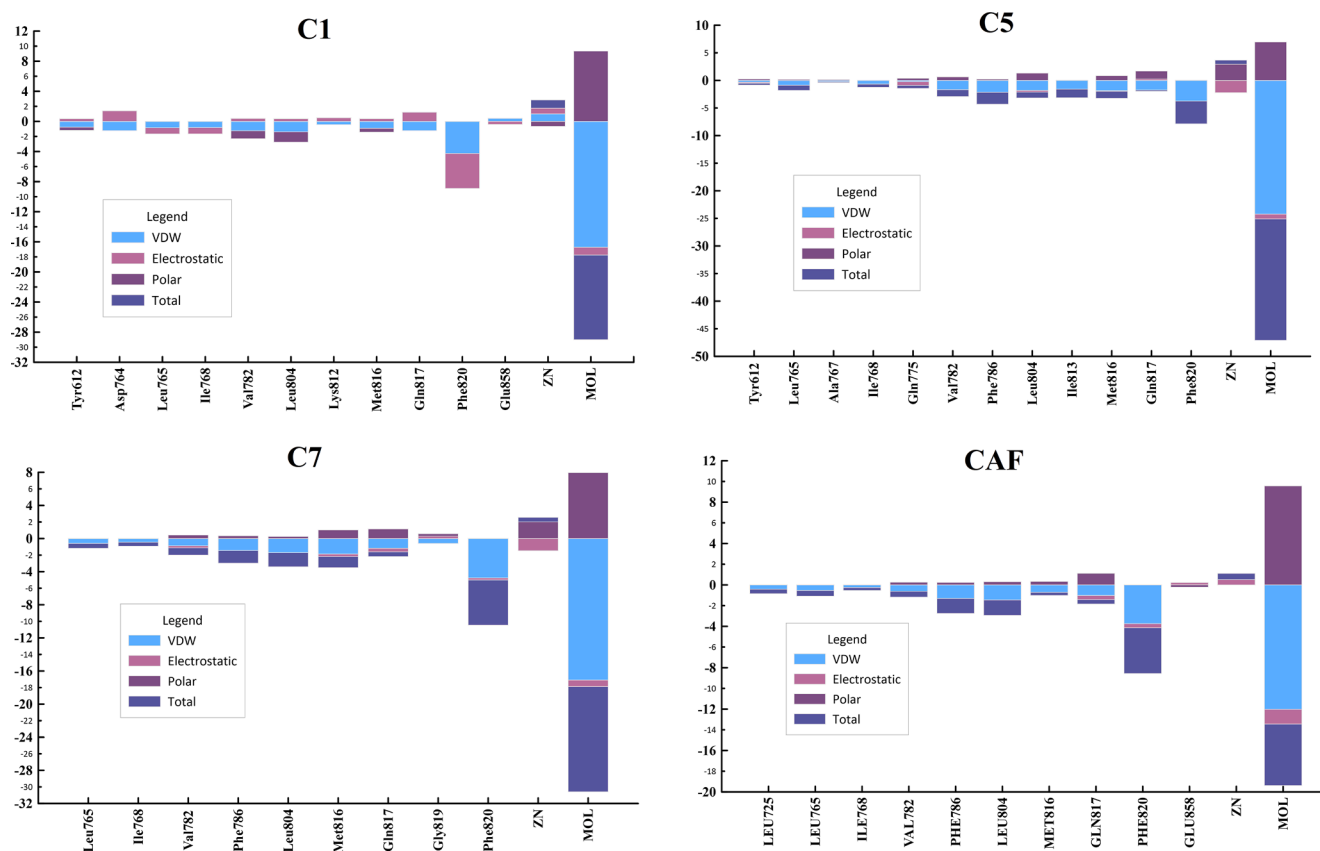


Fig. 10. Bar plot depiction of energy decomposition as the VDW, electrostatic, polar solvation, and total energies for C1, C5, C7, and CAF.

apoptosis [68,69]. Moreover, one of the studied compounds having the heptyl substituent could be utilized in combination with cisplatin, an alkylating agent, to sensitize breast cancer cells. Nevertheless, our derivatives did not show any antioxidant effects. Altogether, our result provided a rationale for using newly developed CAF analogs to target cancer cells exclusively.

Our study had limitations. First, we studied the effects of 8-alkylmercaptocaffeine derivatives on A549 cell lines, two cancerous models for *in vitro* studies that have been reported to have morphological heterogeneity with different proliferative activities [70]. Besides, the KB human mouth cancer cells have been contaminated by Hela cells [71], a human cervical cancer cell line. The other limitation is that we did not perform flow cytometry for analysis of cell cycle and apoptosis. Besides, we did not evaluate the expression of pre- and anti-apoptotic genes that would provide strong evidence on the occurrence of apoptotic cell death. Finally, we performed the docking and MD simulation studies of PDE5A, PDE6A, and PDE9A but did not give the experimental PDE5A, PDE6, and PDE9 inhibition studies.

5. Conclusion

Our results suggested that some synthesized 8-alkylmercaptocaffeine derivatives induce cell death in cancer cells through the cGMP pathway. These findings will help to get a deeper insight into the role of Methylxanthines as useful alternatives to conventional cancer treatments.

CRedit authorship contribution statement

Conceptualization, S.S. (Saman Sargazi); methodology, S.S. (Saman Sargazi), R.S., R.S., S.S., S.M., writing-original draft preparation, S.S. (Saman Sargazi), MS.SR.; writing-review and editing, S.S. (Saman Sargazi), R.S., supervision, S.S. (Saman Sargazi); All authors

have read and agreed to the published version of the manuscript.

Declaration of competing interest

The authors declare that they have no conflict of interest.

Acknowledgments

This work is financially supported by Zahedan University of Medical Sciences, Zahedan, Iran (Grant No: 9585, IR.ZAUMS.REC.1399.294).

Appendix A. Supplementary data

Supplementary data to this article can be found online at <https://doi.org/10.1016/j.bioorg.2021.104900>.

References

- [1] I.-A. Lee, A. Kamba, D. Low, E. Mizoguchi, Novel methylxanthine derivative-mediated anti-inflammatory effects in inflammatory bowel disease, *World J. Gastroenterol.*: WJG 20 (5) (2014) 1127.
- [2] B.B. Fredholm, *Methylxanthines*, Springer Science & Business Media 2010.
- [3] B.G. Katzung, *Basic and clinical pharmacology*, Mc Graw Hill (2012).
- [4] M.S. Rad, S. Maghsoudi, Two-step three-component process for one-pot synthesis of 8-alkylmercaptocaffeine derivatives, *RSC Adv.* 6 (74) (2016) 70335–70342.
- [5] M. Shamsuzzaman, G. Kavita, R. Arunabha, Methylxanthine induced cardiotoxicity and its mechanisms: An experimental study, *Manipal J. Med. Sci.* 1 (2) (2016) 10–19.
- [6] S. Pal, K. Khan, S.P. China, M. Mittal, R. Shrivastava, I. Taneja, Z. Hossain, D. Mandalapu, J.R. Gayen, M. Wahajuddin, Theophylline, a methylxanthine drug induces osteopenia and alters calciotropic hormones, and prophylactic vitamin D treatment protects against these changes in rats, *Toxicol. Appl. Pharmacol.* 295 (2016) 12–25.
- [7] R. Savai, S.S. Pullamsetti, G.-A. Banat, N. Weissmann, H.A. Ghofrani, F. Grimminger, R.T. Schermuly, Targeting cancer with phosphodiesterase inhibitors, *Expert Opin. Invest. Drugs* 19 (1) (2010) 117–131.

- [8] Y. Hou, N. Gupta, P. Schoenlein, E. Wong, R. Martindale, V. Ganapathy, D. Browning, An anti-tumor role for cGMP-dependent protein kinase, *Cancer Lett.* 240 (1) (2006) 60–68.
- [9] S. Naviglio, M. Caraglio, A. Abbruzzese, E. Chiosi, D. Di Gesto, M. Marra, M. Romano, A. Sorrentino, L. Sorvillo, A. Spina, Protein kinase A as a biological target in cancer therapy, *Expert opinion on therapeutic targets* 13 (1) (2009) 83–92.
- [10] R. Saravani, H.R. Galavi, A. Shahraki, Inhibition of phosphodiesterase 5 and increasing the level of cyclic guanosine 3', 5' monophosphate by hydroalcoholic achillea wilhelmsii C. Koch extract in human breast cancer cell lines MCF-7 and MDA-Mb-468, *Breast Cancer: Basic Clin. Res.*, 11 (2017) 1178223417690178.
- [11] R. Saravani, F. Karami-Tehrani, M. Hashemi, M. Aghaei, R. Edalat, Inhibition of phosphodiesterase 9 induces c GMP accumulation and apoptosis in human breast cancer cell lines, MCF-7 and MDA-MB-468, *Cell Prolif.* 45 (3) (2012) 199–206.
- [12] S.H. Francis, K.R. Sekhar, H. Ke, J.D. Corbin, Inhibition of cyclic nucleotide phosphodiesterases by methylxanthines and related compounds, *Springer, Methylxanthines*, 2011, pp. 93–133.
- [13] N. Sugimoto, S. Miwa, Y. Hitomi, H. Nakamura, H. Tsuchiya, A. Yachie, Theobromine, the primary methylxanthine found in Theobroma cacao, prevents malignant glioblastoma proliferation by negatively regulating phosphodiesterase-4, extracellular signal-regulated kinase, Akt/mammalian target of rapamycin kinase, and nuclear factor-kappa B, *Nutr. Cancer* 66 (3) (2014) 419–423.
- [14] J.R. Prasanthi, B. Dasari, G. Marwartha, T. Larson, X. Chen, J.D. Geiger, O. Ghribi, Caffeine protects against oxidative stress and Alzheimer's disease-like pathology in rabbit hippocampus induced by cholesterol-enriched diet, *Free Radical Biol. Med.* 49 (7) (2010) 1212–1220.
- [15] S.D. Varma, K.R. Hegde, Kynurenine-induced photo oxidative damage to lens in vitro: protective effect of caffeine, *Mol. Cell. Biochem.* 340 (1–2) (2010) 49–54.
- [16] P.M. Santos, S.A. Silva, G.C. Justino, A.J. Vieira, Demethylation of theophylline (1, 3-dimethylxanthine) to 1-methylxanthine: the first step of an antioxidising cascade, *Redox Rep.* 15 (3) (2010) 138–144.
- [17] S. Koka, A. Das, F.N. Salloum, R.C. Kukreja, Phosphodiesterase-5 inhibitor tadalafil attenuates oxidative stress and protects against myocardial ischemia/reperfusion injury in type 2 diabetic mice, *Free Radical Biol. Med.* 60 (2013) 80–88.
- [18] J. Milara, A. Navarro, P. Almudiver, J. Lluch, E. Morcillo, J. Cortijo, Oxidative stress-induced glucocorticoid resistance is prevented by dual PDE3/PDE4 inhibition in human alveolar macrophages, *Clin. Exp. Allergy* 41 (4) (2011) 535–546.
- [19] S. Jayakumar, D. Mahendiran, V. Viswanathan, D. Velmurugan, A. Kalilur Rahiman, Heteroscorpionate-based heteroleptic copper (II) complexes: Antioxidant, molecular docking and in vitro cytotoxicity studies, *Appl. Organomet. Chem.* 31 (11) (2017), e3809.
- [20] I. Mármol, J. Quero, M.J. Rodríguez-Yoldi, E. Cerrada, Gold as a Possible Alternative to Platinum-Based Chemotherapy for Colon Cancer Treatment, *Cancers* 11 (6) (2019) 780.
- [21] A. Ohta, M. Sitkovsky, Methylxanthines, inflammation, and cancer: fundamental mechanisms, *Springer, Methylxanthines*, 2011, pp. 469–481.
- [22] S. Uccella, A. Mariani, A. Wang, R. Vierkant, W.A. Cliby, K. Robien, K.E. Anderson, J.R. Cerhan, Intake of coffee, caffeine and other methylxanthines and risk of Type I vs Type II endometrial cancer, *Br. J. Cancer* 109 (7) (2013) 1908–1913.
- [23] E. Petru, G. Boike, B. Sevin, Potentiation of cisplatin cytotoxicity by methylxanthines in vitro, *J. Cancer Res. Clin. Oncol.* 116 (5) (1990) 431–433.
- [24] A. Kakuyamanee Iwazaki, Y. Sadzuka, Effect of methylxanthine derivatives on doxorubicin transport and antitumor activity, *Curr. Drug Metab.* 2 (4) (2001) 379–395.
- [25] G. Ciapetti, E. Cenni, L. Pratelli, A. Pizzoferrato, In vitro evaluation of cell/biomaterial interaction by MTT assay, *Biomaterials* 14 (5) (1993) 359–364.
- [26] T.-C. Chou, P. Talalay, Quantitative analysis of dose-effect relationships: the combined effects of multiple drugs or enzyme inhibitors, *Adv. Enzyme Regul.* 22 (1984) 27–55.
- [27] T.-C. Chou, Theoretical basis, experimental design, and computerized simulation of synergism and antagonism in drug combination studies, *Pharmacol. Rev.* 58 (3) (2006) 621–681.
- [28] M.L. Sargazi, R. Saravani, A. Shahraki, Hydroalcoholic Extract of Levisticum officinale Increases cGMP Signaling Pathway by Down-Regulating PDE5 Expression and Induction of Apoptosis in MCF-7 and MDA-MB-468 Breast Cancer Cell Lines, *Iranian Biomed. J.* 23 (4) (2019) 280.
- [29] A.A. Boligon, R.P. Pereira, A.C. Feltrin, M.M. Machado, V. Janovik, J.B.T. Rocha, M.L. Athayde, Antioxidant activities of flavonol derivatives from the leaves and stem bark of *Scutia buxifolia* Reiss, *Bioresour. Technol.* 100 (24) (2009) 6592–6598.
- [30] H. Ohkawa, N. Ohishi, K. Yagi, Assay for lipid peroxides in animal tissues by thiobarbituric acid reaction, *Anal. Biochem.* 95 (2) (1979) 351–358.
- [31] N.J. Kruger, The Bradford method for protein quantitation, in: *The protein protocols handbook*, Springer, 2009, pp. 17–24.
- [32] T. Hočevar, J. Demšar, Computation of graphlet orbits for nodes and edges in sparse graphs, *J. Stat. Softw.* 71 (1) (2016) 1–24.
- [33] K.Y. Zhang, G.L. Card, Y. Suzuki, D.R. Artis, D. Fong, S. Gillette, D. Hsieh, J. Neiman, B.L. West, C. Zhang, A glutamine switch mechanism for nucleotide selectivity by phosphodiesterases, *Mol. Cell* 15 (2) (2004) 279–286.
- [34] Y. Wu, Q. Zhou, T. Zhang, Z. Li, Y.-P. Chen, P. Zhang, Y.-F. Yu, H. Geng, Y.-J. Tian, C. Zhang, Discovery of Potent, Selective, and Orally Bioavailable Inhibitors against Phosphodiesterase-9, a Novel Target for the Treatment of Vascular Dementia, *J. Med. Chem.* 62 (8) (2019) 4218–4224.
- [35] Y. Gao, G. Eskici, S. Ramachandran, F. Poitevin, A.B. Seven, O. Panova, G. Skiniotis, R.A. Cerione, Structure of the Visual Signaling Complex between Transducin and Phosphodiesterase 6, *Mol. Cell* 80(2) (2020) 237–245. e4.
- [36] W. Yang, B.T. Riley, X. Lei, B.T. Porebski, I. Kass, A.M. Buckle, S. McGowan, Generation of AMBER force field parameters for zinc centres of M1 and M17 family aminopeptidases, *J. Biomol. Struct. Dyn.* 36 (10) (2018) 2595–2604.
- [37] D.A. Case, T. Darden, T. Cheatham, C.L. Simmerling, J. Wang, R.E. Duke, R. Luo, M. Crowley, R.C. Walker, W. Zhang, Amber 10, University of California, 2008.
- [38] J. Wang, R.M. Wolf, J.W. Caldwell, P.A. Kollman, D.A. Case, Development and testing of a general amber force field, *J. Comput. Chem.* 25 (9) (2004) 1157–1174.
- [39] J.A. Maier, C. Martinez, K. Kasavajhala, L. Wickstrom, K.E. Hauser, C. Simmerling, ff14SB: improving the accuracy of protein side chain and backbone parameters from ff99SB 11 (8) (2015) 3696–3713.
- [40] E. Vanqualef, S. Simon, G. Marquant, E. Garcia, G. Klimerak, J.C. Delepine, P. Cieplak, F.-Y. Dupradeau, RED Server: a web service for deriving RESP and ESP charges and building force field libraries for new molecules and molecular fragments, *Nucl. Acids Res.* 39(suppl_2) (2011) W511–W517.
- [41] R.W. Hockney, J.W. Eastwood, Computer simulation using particles, *crc Press*, 1988.
- [42] T. Darden, D. York, L. Pedersen, Particle mesh Ewald: An N- log (N) method for Ewald sums in large systems, *J. Chem. Phys.* 98 (12) (1993) 10089–10092.
- [43] B. Hess, H. Bekker, H.J. Berendsen, J.G. Fraaije, LINCS: a linear constraint solver for molecular simulations, *J. Comput. Chem.* 18 (12) (1997) 1463–1472.
- [44] N. Goga, A. Rzepiela, A. De Vries, S. Marrink, H. Berendsen, Efficient algorithms for Langevin and DPD dynamics, *J. Chem. Theory Comput.* 8 (10) (2012) 3637–3649.
- [45] C. Wang, P.H. Nguyen, K. Pham, D. Huynh, T.B.N. Le, H. Wang, P. Ren, R. Luo, Calculating protein–ligand binding affinities with MMPBSA, *Method Error Anal.* 37 (27) (2016) 2436–2446.
- [46] H. Sun, L. Duan, F. Chen, H. Liu, Z. Wang, P. Pan, F. Zhu, J.Z. Zhang, T. Hou, Assessing the performance of MM/PBSA and MM/GBSA methods. 7. Entropy effects on the performance of end-point binding free energy calculation approaches 20 (21) (2018) 14450–14460.
- [47] Y.S. Kiani, K.E. Ranaghan, I. Jabeen, A.J. Mulholland, Molecular Dynamics Simulation Framework to Probe the Binding Hypothesis of CYP3A4, *Inhibitors* 20 (18) (2019) 4468.
- [48] R. De Paris, C.V. Quevedo, D.D. Ruiz, O. Norberto de Souza, R.C.J.C.i. Barros, neuroscience, Clustering molecular dynamics trajectories for optimizing docking experiments, 2015 (2015).
- [49] Z. Wang, H. Sun, X. Yao, D. Li, L. Xu, Y. Li, S. Tian, T. Hou, Comprehensive evaluation of ten docking programs on a diverse set of protein–ligand complexes: the prediction accuracy of sampling power and scoring power, *PCCP* 18 (18) (2016) 12964–12975.
- [50] H. Wang, X. Luo, M. Ye, J. Hou, H. Robinson, H. Ke, Insight into binding of phosphodiesterase-9A selective inhibitors by crystal structures and mutagenesis, *J. Med. Chem.* 53 (4) (2010) 1726–1731.
- [51] M. Feig, A. Onufriev, M.S. Lee, W. Im, D.A. Case, C.L. Brooks III, Performance comparison of generalized born and Poisson methods in the calculation of electrostatic solvation energies for protein structures, 25(2) (2004) 265–284.
- [52] J. Srinivasan, M.W. Trevathan, P. Beroza, D.A. Case, Application of a pairwise generalized Born model to proteins and nucleic acids: inclusion of salt effects, *Theor. Chem. Acc.* 101 (6) (1999) 426–434.
- [53] J.B. Axelsen, S. Andersen, X.-Q. Sun, S. Ringgaard, J.A. Hyldebrandt, K. Kurakula, M.-J. Goumans, F.S. de Man, J.E. Nielsen-Kudsk, H.-J. Bogaard, Effects of 6-mercaptopurine in pressure overload induced right heart failure, *PLoS ONE* 14 (11) (2019), e0225122.
- [54] J.J. McDonald, G. Stöhrer, G.B. Brown, Oncogenic purine N-oxide derivatives as substrates for sulfotransferase, *Cancer Res.* 33 (12) (1973) 3319–3323.
- [55] Y. Ohsaki, S. Ishida, T. Fujikane, K. Kikuchi, Pentoxifylline potentiates the antitumor effect of cisplatin and etoposide on human lung cancer cell lines, *Oncology* 53 (4) (1996) 327–333.
- [56] Y. Oda, M. Hidaka, A. Suzuki, Caffeine Has a Synergistic Anticancer Effect with Cisplatin via Inhibiting Fanconi anemia group d2 protein monoubiquitination in hepatocellular carcinoma cells, *Biol. Pharm. Bull.* (2017) b17–00457.
- [57] H. Liu, Y. Zhou, L. Tang, Caffeine induces sustained apoptosis of human gastric cancer cells by activating the caspase-9/caspase-3 signalling pathway, *Mol. Med. Rep.* 16 (3) (2017) 2445–2454.
- [58] S. Mostert, W. Mentz, A. Petzer, J.J. Bergh, J.P. Petzer, Inhibition of monoamine oxidase by 8-[(phenylethyl) sulfanyl] caffeine analogues, *Bioorg. Med. Chem.* 20 (24) (2012) 7040–7050.
- [59] S. Rivara, G. Piersanti, F. Bartocchini, G. Diamantini, D. Pala, T. Riccioni, M.A. Stasi, W. Cabri, F. Borsini, M. Mor, Synthesis of (E)-8-(3-chlorostyryl) caffeine analogues leading to 9-deazaxanthine derivatives as dual A2A antagonists/MAO-B inhibitors, *J. Med. Chem.* 56 (3) (2013) 1247–1261.
- [60] G. Krutovskikh, M. Kolesova, A. Rusanov, L. Vartanyan, M. Shagoyan, Radioprotective properties of mercaptocaffeine derivatives, *Pharm. Chem. J.* 9 (4) (1975) 234–236.
- [61] J. Mitkov, N. Danchev, I. Nikolova, A. Zlatkov, Synthesis and brain antihypoxic activity of some aliphatic and arylaliphatic amides of caffeine-8-thioglycolic acid, *Acta Pharmaceutica* 57 (3) (2007) 361.
- [62] M.N.S. Rad, S. Behrouz, H. Najafi, N7-Tosyltheophylline (TsTh): a highly efficient reagent for the one-pot synthesis of N7-alkyltheophyllines from alcohols, *Synthesis* 46 (10) (2014) 1380–1388.
- [63] G. Duranti, R. Ceci, P. Sgrò, S. Sabatini, L. Di Luigi, Influence of the PDE5 inhibitor tadalafil on redox status and antioxidant defense system in C2C12 skeletal muscle cells, *Cell Stress Chaperones* 22 (3) (2017) 389–396.

- [64] S. Azam, N. Hadi, N.U. Khan, S.M. Hadi, Antioxidant and prooxidant properties of caffeine, theobromine and xanthine, *Med. Sci. Monit.* 9 (9) (2003) BR325–BR330.
- [65] S. Catalano, S. Panza, G. Augimeri, C. Giordano, R. Malivindi, L. Gelsomino, S. Marsico, F. Giordano, B. Gyórfy, D. Bonofiglio, Phosphodiesterase 5 (PDE5) Is Highly Expressed in Cancer-Associated Fibroblasts and Enhances Breast Tumor Progression, *Cancers* 11 (11) (2019) 1740.
- [66] L. Booth, J.L. Roberts, N. Cruickshanks, A. Conley, D.E. Durrant, A. Das, P. B. Fisher, R.C. Kukreja, S. Grant, A. Poklepovic, Phosphodiesterase 5 inhibitors enhance chemotherapy killing in gastrointestinal/genitourinary cancer cells, *Mol. Pharmacol.* 85 (3) (2014) 408–419.
- [67] G.A. Piazza, A. Ward, X. Chen, Y. Maxuitenko, A. Coley, N.S. Aboeella, D. J. Buchsbaum, M.R. Boyd, A.B. Keeton, G. Zhou, PDE5 and PDE10 inhibition activates cGMP/PKG signaling to block Wnt/ β -catenin transcription, cancer cell growth, and tumor immunity, *Drug Discovery Today* (2020).
- [68] B. Zhu, L. Vemavarapu, W.J. Thompson, S.J. Strada, Suppression of cyclic GMP-specific phosphodiesterase 5 promotes apoptosis and inhibits growth in HT29 cells, *J. Cell. Biochem.* 94 (2) (2005) 336–350.
- [69] T.C. Peak, A. Richman, S. Gur, F.A. Yafi, W.J. Hellstrom, The role of PDE5 inhibitors and the NO/cGMP pathway in cancer, *Sexual Med. Rev.* 4 (1) (2016) 74–84.
- [70] M.V. Croce, A.G. Colussi, M.R. Price, A. Segal-Eiras, Identification and characterization of different subpopulations in a human lung adenocarcinoma cell line (A549), *Pathol. Oncol. Res.* 5 (3) (1999) 197–204.
- [71] M. Lacroix, Persistent use of “false” cell lines, *Int. J. Cancer* 122 (1) (2008) 1–4.